

Quasidynamical Symmetry in an Interacting Boson Model Phase Transition

D. J. Rowe

Department of Physics, University of Toronto, Toronto, Ontario, Canada M5S 1A7

(Received 5 February 2004; published 16 September 2004)

The apparent persistence of symmetry in the face of strong symmetry-breaking interactions is examined in a many-boson model. The model exhibits a transition between two phases associated with U(5) and O(6) symmetries, respectively, as the value of a control parameter progresses from 0 to 1. The remarkable fact is that, in spite of strong mixing of the symmetries for intermediate values of the control parameter, the model continues to exhibit the characteristics of its closest symmetry limit for all but a relatively narrow transition region that becomes progressively narrower as the boson number increases. This phenomenon is explained in terms of quasidynamical symmetry.

DOI: 10.1103/PhysRevLett.93.122502

PACS numbers: 21.60.Fw, 03.65.Fd, 05.70.Fh, 21.10.Re

Although designed for use with finite many-particle systems, nuclear models of phase transitions [1–6] can often be applied to large, even infinite, numbers of particles. They then become relevant for the study of phase transitions in more general systems. The interacting boson model (IBM) [7] comprises a system of N two-state bosons: a lower-energy $L = 0$ (s -boson) state and a higher-energy $L = 2$ (d -boson) state with five orientations. When the bosons are noninteracting, they form a spherically symmetric s -boson condensate. As an interaction is turned on, the condensate is increasingly depleted until a point is reached at which a new nonspherical phase begins to develop. In this Letter, a particular case of the IBM is examined for several relatively large values of N and inferences are drawn about its $N \rightarrow \infty$ limit.

The model exhibits a number of remarkable properties: (i) the phases on either side of a transition region appear to be much more distinct and defined than could reasonably be expected for finite values of N ; (ii) as N increases, the transition region shrinks and develops a critical point as $N \rightarrow \infty$; (iii) the symmetries associated with the two phases appear to persist in spite of relatively strong symmetry-breaking interactions. The latter phenomenon has been observed in several other model systems and is interpreted in terms of *quasidynamical symmetry* [2,8,9]. The quasidynamical symmetries of the present model are explained in terms of approximations which become exact as $N \rightarrow \infty$.

Quasidynamical symmetry is an expression of the possibility that a subset of physical data may exhibit all the properties that would result if the system had a symmetry which, in fact, it does not have. The existence of *embedded representations* [10] shows in precise mathematical terms that this can happen. Its realization would be demonstrated experimentally, if it could be shown that a significant subset of observed data exhibit all the properties of a symmetry but further, perhaps more detailed data, reveal the symmetry to be badly broken.

Creation and annihilation operators for the IBM bosons are denoted by $\{s^\dagger, d_\nu^\dagger\}$ and $\{s, d_\nu\}$ with $\nu = 0, \pm 1, \pm 2$. They satisfy the commutation relations

$$[s, s^\dagger] = 1, \quad [d_\nu^\mu, d_\nu^\dagger] = \delta_{\mu\nu}, \quad [s, d_\nu^\dagger] = [d_\nu, s^\dagger] = 0. \quad (1)$$

Note that upper and lower indices are used to distinguish contravariant and covariant spherical tensors which enable the scalar product of spherical tensors, for example, to be expressed by $d \cdot d = \sum_\nu d_\nu^\nu d_\nu$ with

$$d_\nu = (-1)^\nu d_\nu^\nu. \quad (2)$$

The Hilbert space of the IBM can be realized as a subspace of states of N quanta of a six-dimensional harmonic oscillator. Thus, it carries an irrep (irreducible representation) of the group U(6). The group U(6) has several subgroups and different phases of the model can be associated with Hamiltonians that are invariant under different subgroups. We consider the Hamiltonian [4,7]

$$\hat{H}(\alpha) = (1 - \alpha)\hat{H}_1 + \alpha\hat{H}_2, \quad (3)$$

with control parameter α , where \hat{H}_1 is the U(5)-invariant d -boson number operator and \hat{H}_2 is O(6) invariant:

$$\hat{H}_1 = \hat{n} = \sum_\nu d_\nu^\dagger d_\nu, \quad \hat{H}_2 = \frac{1}{N} \hat{S}_+ \hat{S}_-, \quad (4)$$

$$\hat{S}_+ = \frac{1}{2}(d^\dagger \cdot d^\dagger - s^\dagger s^\dagger), \quad \hat{S}_- = \frac{1}{2}(d \cdot d - ss). \quad (5)$$

An electric quadrupole moment operator is represented in the model by

$$\hat{Q}_\nu = \frac{Z}{\sqrt{N}}(d_\nu^\dagger s + s^\dagger d_\nu), \quad \nu = 0, \pm 1, \pm 2, \quad (6)$$

where Z is a norm factor (can be thought of as charge).

The physical content of the model is revealed, following Refs. [4,11], by interpreting the coherent-state energy function $E_\alpha(q) = \langle \phi(q) | \hat{H}(\alpha) | \phi(q) \rangle$, where

$$|\phi(q)\rangle = (1 - \beta^2)^{N/2} \exp\left[\frac{1}{\sqrt{1 - \beta^2}} \sum_\nu q^\nu d_\nu^\dagger s\right] |\phi\rangle \quad (7)$$

with $\beta^2 = \sum_\nu |q^\nu|^2$, as the potential energy of the classical counterpart [12] of the Hamiltonian $\hat{H}(\alpha)$. E_α is given, to within an unimportant constant, by

$$E_\alpha(q) = V_\alpha(\beta) = N \left[\beta^2 + \alpha(-2\beta^2 + \beta^4) + O\left(\frac{1}{N}\right) \right] \quad (8)$$

and shown in Fig. 1. For $\alpha \leq 0.5$, the minimum of the potential is at $\beta = 0$, and for $\alpha > 0.5$ it is at a nonzero value of β that increases monotonically with α . Note that V_α depends only on $\beta^2 = q \cdot q$; this is because it is invariant under a group of SO(5) rotations as also is the Hamiltonian $\hat{H}(\alpha)$; the latter depends only on SO(5) scalar combinations $d^\dagger \cdot d^\dagger$, $d^\dagger \cdot d$, and $d \cdot d$ of the d -boson operators. Thus, for $\alpha > 0.5$, E_α has the shape of a five-dimensional Mexican hat. Now the parameters $\{q^\nu\}$ define the quadrupole moments of the coherent state $|\phi(q)\rangle$ such that the quadrupole deformation is zero when $\beta = 0$ and maximum when $\beta = 1$. Thus, the classical potential V_α suggests that, as α is increased, the system will remain in a spherical equilibrium shape and have vibrational excitations for $\alpha < 0.5$ after which it will adopt a deformed equilibrium shape, in the manner of a second-order phase transition, and acquire rotational as well as vibrational excitations. The following results show the extent to which the above classical perspective is realized in a full quantum-mechanical treatment.

The energy-level spectrum and the electric quadrupole transitions for the Hamiltonian $\hat{H}(\alpha)$ have been calculated as functions of α over the range $0 \leq \alpha \leq 1$. The model is analytically solvable in its ($\alpha = 0$) U(5)- and ($\alpha = 1$) O(6)-symmetry limits. The numerically computed results for intermediate values of α are determined by use of a simple $SU(1, 1)^s + SU(1, 1)^d$ spectrum generating algebra with basis elements

$$\hat{S}_+^s = \frac{1}{2}s^\dagger s^\dagger, \quad \hat{S}_-^s = \frac{1}{2}ss, \quad \hat{S}_0^s = \frac{1}{4}(s^\dagger s + ss^\dagger), \quad (9)$$

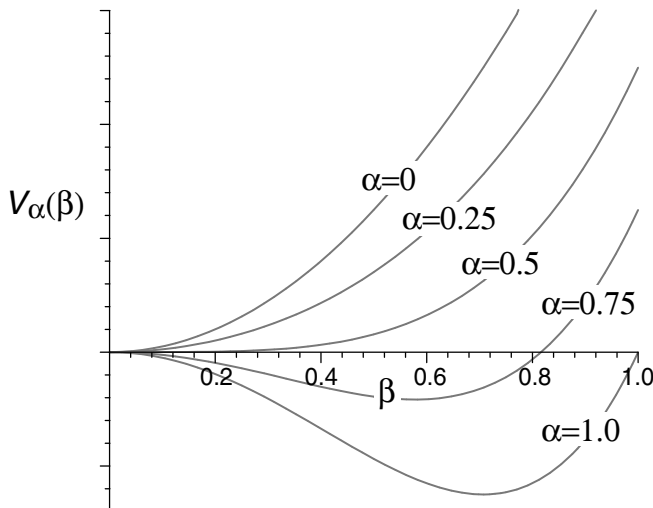


FIG. 1. The energy function $V_\alpha(\beta)$ for different values of α .

$$\hat{S}_+^d = \frac{1}{2}d^\dagger \cdot d^\dagger, \quad \hat{S}_-^d = \frac{1}{2}d \cdot d, \quad \hat{S}_0^d = \frac{1}{4}(d^\dagger \cdot d + d \cdot d^\dagger). \quad (10)$$

Energy levels, labeled by an SO(5) quantum number ν , and E2 transition rates for decay of the first excited state of the model are shown as functions of α in Figs. 2 and 3.

A striking result of Figs. 2 and 3 is that the model appears to hold onto its U(5) symmetry for $0 \leq \alpha \leq 0.3$ and to its O(6) symmetry for $0.8 \leq \alpha \leq 1$ and that there is a relatively rapid transition between the states of one symmetry to the other in the intermediate region. Insight into the actual evolution of the model states with increasing α is given by approximate solutions which predict a phase transition and do so with increasing accuracy as N increases. We consider the familiar random phase approximation (RPA) for $0 \leq \alpha \leq 0.5$ and a shifted harmonic approximation (SHA) for $0.5 \leq \alpha \leq 1$.

For small values of α , the RPA gives quasiboson excitation operators

$$D_\nu^\dagger = (x d_\nu^\dagger s - y s^\dagger d_\nu) / \sqrt{N}, \quad (11)$$

with coefficients that satisfy a 2×2 eigenvector equation of the non-Hermitian form

$$\begin{pmatrix} A & B \\ -B & -A \end{pmatrix} \begin{pmatrix} x \\ y \end{pmatrix} = \varepsilon \begin{pmatrix} x \\ y \end{pmatrix}, \quad (12)$$

with A and B given, in the double-commutator equations of motion formalism [13], by

$$A = \frac{1}{N} \langle \phi | [s^\dagger d^\nu, [H(\alpha), d_\nu^\dagger s]] | \phi \rangle = \left(1 - \frac{3}{2} \alpha \right), \quad (13)$$

$$B = -\frac{1}{N} \langle \phi | [s^\dagger d^\nu, [H(\alpha), s^\dagger d_\nu]] | \phi \rangle = -\frac{1}{2} \alpha; \quad (14)$$

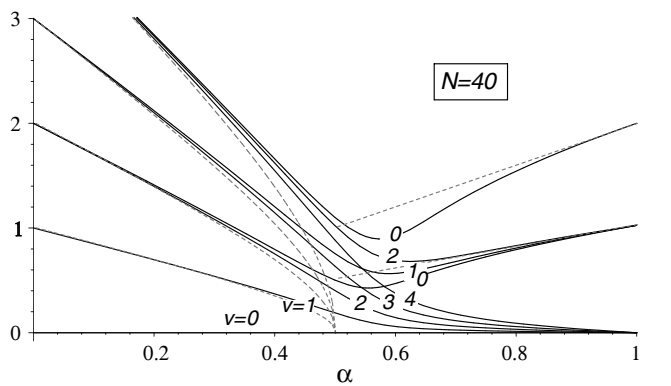


FIG. 2. Excitation energies of the Hamiltonian $\hat{H}(\alpha)$ as a function of α . The continuous lines show precise, numerically computed energies. The dotted lines are results of an RPA calculation (for $\alpha < 0.5$) and an SHA calculation (for $\alpha > 0.5$). Note that N levels coalesce to form a degenerate ground state, and $N - m$ levels coalesce to the m th excited multiplet, as $\alpha \rightarrow 1$. Thus, the level density is much higher in the mid- α region than this figure would suggest.

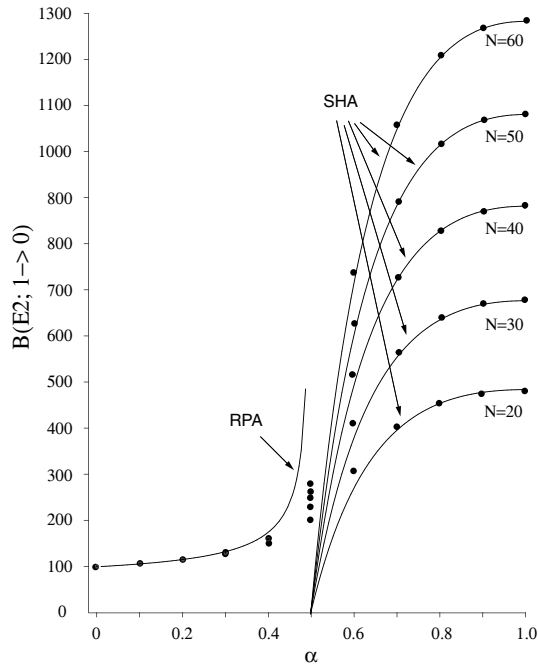


FIG. 3. $B(E2)$ transition rates for decay of the first excited $\nu = 1$ energy level to the ground state for various values of N expressed in units such that $B(E2; 1 \rightarrow 0) = 100$ in the $U(5)$ ($\alpha = 0$) limit. The continuous lines for $\alpha \leq 0.5$ are for the RPA and those for $\alpha \geq 0.5$ are for the SHA. The dots are precise (numerically computed) results.

$|\phi\rangle$ is the uncorrelated ground state given by the s -boson condensate $|\phi\rangle = (s^\dagger)^N |0\rangle / \sqrt{N!}$. The RPA energy spectrum, $n\epsilon$ with $\epsilon = \sqrt{(1-\alpha)(1-2\alpha)}$, is shown in Fig. 2 as dotted lines for $\alpha \leq 0.5$. It predicts a collapse of the excitation energies to zero and, in Fig. 3, a divergence of the $E2$ transition rate for decay of the $\nu = 1$ first excited state as $\alpha \rightarrow 0.5$. Thus, the RPA predicts a phase transition at $\alpha_{\text{crit}} = 0.5$ in accord with the Thouless Hartree-Fock stability condition [14].

The RPA has been applied previously to the IBM [15]. In the present context it is particularly useful for two reasons: (i) it is known to become increasingly accurate as the particle number approaches an infinite value and (ii) when it gives accurate results, it implies the existence of a quasi- $U(5)$ symmetry. As a quasiboson approximation, the RPA is equivalent to the Bogolyubov approximation of replacing the s -boson operators, s^\dagger and s , by the c number \sqrt{N} ; this approximation, which can be expressed more elegantly as a Wigner contraction, gives increasingly accurate results as $N \rightarrow \infty$. The RPA transformation of Eq. (11) is then seen as the $SU(1, 1)$ transformation

$$d_\nu^\dagger \rightarrow D_\nu^\dagger = x d_\nu^\dagger - y d_\nu, \quad x^2 - y^2 = 1, \quad (15)$$

that brings the Hamiltonian and electric quadrupole operators to the forms

$$\hat{H}_{\text{RPA}} = \epsilon \sum_\nu D_\nu^\dagger D_\nu + \text{const}, \quad (16)$$

$$\hat{Q}_\nu^{\text{RPA}} = Z'(D_\nu^\dagger + D_\nu), \quad \nu = 0, \pm 1, \pm 2. \quad (17)$$

This reveals the RPA as an approximation with a $U(5)$ dynamical symmetry in spite of the fact that the states of the IBM system it describes are linear combinations of states from inequivalent irreps of the $U(5) \subset U(6)$ symmetry group of the $\alpha = 0$ limit. Thus, in the domain in which the RPA gives accurate results, its $U(5)$ symmetry is a quasidynamical symmetry of the IBM.

I now consider the nature of the eigenstates of $\hat{H}(\alpha)$ for $\alpha > 0.5$. Figure 4 shows the numerically computed coefficients in the expansion $|\Psi_{\nu LM}\rangle = \sum_n C_{n\nu\nu} |n\nu LM\rangle$ of the lowest and first excited $\nu = 0$ eigenstates of $\hat{H}(\alpha)$ for $\alpha = 1.0$ and 0.75 in a basis $\{|n\nu LM\rangle\}$ which diagonalizes the Hamiltonian $\hat{H}(\alpha = 0) = \hat{n}$ (n is the d -boson number). The coefficients for other values of the $SO(5)$ quantum number ν (which distinguishes the many energy levels that coalesce into a common level at $\alpha = 1$) are determined to be essentially identical to those of $\nu = 0$ when $\nu \ll N$.

Figure 4 shows that the numerically computed coefficients, given by dots, are fitted quite precisely by suitably placed harmonic oscillator wave functions (shown by continuous lines). In fact, all the above-mentioned properties of the computed wave functions, including the parameters of the harmonic oscillator functions shown, were derived in a *shifted harmonic approximation*. This approximation is defined by writing down the eigenvector equation for the coefficients $C_{n\nu\nu} = \langle n\nu LM | \Psi_{\nu LM} \rangle$ of the eigenstates $\{|\Psi_{\nu LM}\rangle\}$ of $\hat{H}(\alpha)$ and using finite difference methods to convert it into a differential equation for the functions

$$\Psi_{\nu\nu}(x) = C_{n\nu\nu}, \quad x = \frac{1}{2}(n - N/2). \quad (18)$$

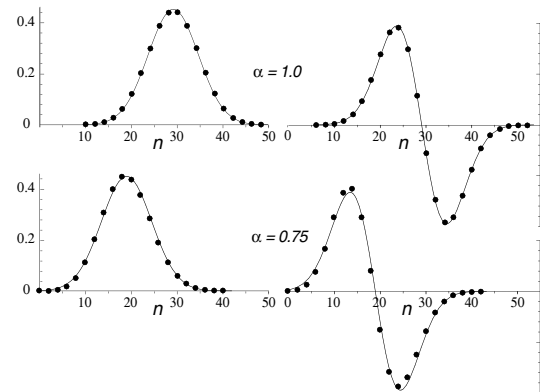


FIG. 4. Wave functions for the $N = 60$ ground state and first excited $\nu = 0$ state for $\alpha = 1$ and 0.75 . The dots give the coefficients of the states in a basis of d -boson number n . The continuous lines are harmonic oscillator wave functions.

The result is a set of harmonic oscillator equations for wave functions with centroids and widths that accurately fit the numerically computed values of the coefficients for α larger than the values for which the system is in the transition region; this is illustrated in Fig. 4. The predictions of the SHA for energy levels are shown for $N = 40$ in Fig. 2 and for $E2$ transition rates in Fig. 3 for several values of N ; they are likewise seen to be accurate for α above the transition region.

The significance of the shifting of the wave packets, seen in Fig. 4, can be simply understood. In a representation in which the d -boson number operator \hat{n} is diagonal, the inclusion of a term in the Hamiltonian proportional to $\hat{H}_1 = \hat{n}$ simply acts as a Lagrange multiplier to shift the centroid of the wave function to a new mean value of n . So long as a shifted wave function remains within the $n = 0, \dots, N$ range, its form remains essentially unchanged. Thus, the SHA starts to break down at the value of α for which a wave function starts to have nonzero values at the $n = 0$ boundary. From a knowledge of the predicted widths and centroids of the SHA, it is easy to predict the point at which this happens for any given value of N . It is found that the lower limit of validity of the SHA approaches the critical value $\alpha_c = 0.5$ as $N \rightarrow \infty$.

As will be shown in a more complete publication to follow, the SHA for each value of α is an algebraic model with an $O(6)$ dynamical symmetry that mimics the $O(6)$ dynamical symmetry of the IBM $\alpha = 1$ limit. However, as already seen from Fig. 4, the IBM states do not remain unchanged as α decreases; in fact, they become linear combinations of states from different $O(6)$ irreps. Thus, the $O(6)$ dynamical symmetry of the SHA is a quasidynamical symmetry of the IBM in the domain in which it gives accurate results.

Some readers (especially nuclear physicists) will find it useful to note that it is possible to add terms proportional to the $SO(5)$ and $SO(3)$ Casimir operators to the Hamiltonian $\hat{H}(\alpha)$. This would split the degeneracies of the levels shown in the figures. However, because $\hat{H}(\alpha)$ is both $SO(5)$ and $SO(3)$ invariant, such added terms would be diagonal for all α . Thus, they would obscure but not change any of the above conclusions in any way. On the contrary, it is easy to see that considerable improvement to the RPA and SHA results could be achieved, without breaking their respective $U(5) \supset SO(5)$ and $O(6) \supset SO(5)$ dynamical symmetries, by adding terms in the $SO(5)$ Casimir operator to their effective Hamiltonians.

A primary result of the above analysis is to make a precise association of $U(5)$ and $O(6)$ symmetries, respectively, with the spherical and deformed phases of the IBM Hamiltonian $\hat{H}(\alpha)$ even though these symmetries are badly broken in a conventional sense. One can think of the evolution of the low-energy states of the model as they progress through the phase transition in terms of the evolution of a quasidynamical group. In pictorial terms,

the effect of a symmetry-breaking interaction is primarily to distort the dynamical symmetry, rather than break it until there comes a point at which it can be distorted no more. At this point the symmetry really starts to break up; the system enters the transition region and, as it emerges on the other side, a new quasidynamical symmetry associated with the other phase begins to develop.

An interesting question that remains concerns the recent suggestion [4] that a new type of symmetry might develop right at the critical point. This suggests that an interesting sequel to the present investigation will be an exploration of the ways the properties of the system in the transition domain evolve as a function of the boson number N .

The author thanks J. L. Wood for helpful suggestions.

-
- [1] H. Chen, J. R. Brownstein, and D. J. Rowe, *Phys. Rev. C* **42**, 1422 (1990); H. Chen, T. Song, and D. J. Rowe, *Nucl. Phys. A* **582**, 181 (1995).
 - [2] D. J. Rowe, C. Bahri, and W. Wijesundera, *Phys. Rev. Lett.* **80**, 4394 (1998); C. Bahri, D. J. Rowe, and W. Wijesundera, *Phys. Rev. C* **58**, 1539 (1998).
 - [3] R. F. Casten and N. V. Zamfir, *Phys. Rev. Lett.* **85**, 3584 (2000).
 - [4] F. Iachello, *Phys. Rev. Lett.* **85**, 3580 (2000); **87**, 052502 (2001); **91**, 132502 (2003).
 - [5] J. Jolie *et al.*, *Phys. Rev. Lett.* **89**, 182502 (2002).
 - [6] A. Leviatan and J. N. Ginocchio, *Phys. Rev. Lett.* **90**, 212501 (2003).
 - [7] A. Arima and F. Iachello, *Ann. Phys. (N.Y.)* **99**, 253 (1976); **111**, 201 (1978); O. Scholten, A. Arima, and F. Iachello, *Ann. Phys. (N.Y.)* **115**, 325 (1978); F. Iachello and A. Arima, *The Interacting Boson Model* (Cambridge University Press, Cambridge, 1987).
 - [8] J. Carvalho, R. Le Blanc, M. Vassanji, D. J. Rowe, and J. McGrory, *Nucl. Phys. A* **452**, 240 (1986); D. J. Rowe, P. Rochford, and J. Repka, *J. Math. Phys. (N.Y.)* **29**, 572 (1988); P. Rochford and D. J. Rowe, *Phys. Lett. B* **210**, 5 (1988); C. Bahri and D. J. Rowe, *Nucl. Phys. A* **662**, 125 (2000).
 - [9] D. J. Rowe, in *Computational and Group Theoretical Methods in Nuclear Physics, Proceedings of the Symposium in Honor of Jerry P. Draayer's 60th Birthday, Playa del Carmen, Mexico, 2003*, edited by O. Castaños, J. Escher, J. Hirsch, S. Pittel, and G. Stoicheva (World Scientific, Singapore, 2004).
 - [10] D. J. Rowe, P. Rochford, and J. Repka, *J. Math. Phys. (N.Y.)* **29**, 572 (1988); P. Rochford and D. J. Rowe, *Phys. Lett. B* **210**, 5 (1988).
 - [11] A. E. L. Dieperink, O. Scholten, and F. Iachello, *Phys. Rev. Lett.* **44**, 1747 (1980); O. S. Roosmalen and A. E. L. Dieperink, *Phys. Lett.* **100B**, 299 (1981).
 - [12] R. Gilmore, *J. Math. Phys. (N.Y.)* **20**, 891 (1979); S. D. Bartlett and D. J. Rowe, *J. Phys. A* **36**, 1683 (2003).
 - [13] D. J. Rowe, *Rev. Mod. Phys.* **40**, 153 (1968).
 - [14] D. J. Thouless, *Nucl. Phys.* **21**, 225 (1960).
 - [15] O. S. van Roosmalen and A. E. L. Dieperink, *Ann. Phys. (N.Y.)* **139**, 198 (1982).